Organic & Biomolecular Chemistry

PAPER

View Article Online
View Journal | View Issue

Cite this: *Org. Biomol. Chem.*, 2017, **15**, 2422

Mechanistic investigations of the asymmetric hydrosilylation of ketimines with trichlorosilane reveals a dual activation model and an organocatalyst with enhanced efficiency†

X. Li, A. T. Reeder, F. Torri, H. Adams and S. Jones*

Received 18th November 2016,
Accepted 21st February 2017

DOI: 10.1039/c6ob02537d

rsc.li/obc

Structural probes used to help elucidate mechanistic information of the organocatalyzed asymmetric ketimine hydrosilylation have revealed a new catalyst with unprecedented catalytic activity, maintaining adequate performance at 0.01 mol% loading. A new 'dual activation' model has been proposed that relies on the presence of both a Lewis basic and Brønsted acidic site within the catalyst architecture.

Introduction

The organocatalyzed asymmetric hydrosilylation of ketimines provides an effective method to prepare chiral amines in good yield and enantioselectivity. Since the first chiral Lewis-base derived catalyst was reported in 2001,[1] there have been many variants of catalyst prepared and evaluated;[2,3] selected examples include formamides,[4–7] sulfinimides,[8,9] pyridines,[10–12] and organophosphorus compounds.[13–15] The main focus of research from this group has been using an imidazole derived catalyst that has been shown to function as efficiently as the reported analogous picolinoyl series,[16] in addition to being amenable to reductive amination protocols.[17] Despite it being more than a decade since the first asymmetric catalysts for this type of transformation were reported, mechanistic data and insights have been sporadic, and only tentative models have been put forward to explain the selectivity.[18] The most comprehensive study to date is that put forward by Malkov *et al.*,[19] crucially noting the dependence of adventitious Brønsted acids to ensure the success of these reactions. Given the scarcity of mechanistic detail for these catalytic processes, a more in depth structural analysis of the imidazole catalyst system developed in these laboratories has now been conducted, providing new insights into the mechanism of this process, and has delivered a new catalyst with even higher activity.

Results and discussion

The role of the Lewis basic amide in relation to the imidazole ring system was first investigated. A series of *N*-substituted imidazoles and their corresponding dimethylamides were prepared. 1-Methylimidazole **1** is commercially available, whereas 1-*tert*-butylimidazole **2** was prepared by condensing a mixture of glyoxal, aqueous formaldehyde, aqueous ammonia and *tert*-butylamine.[20] These were converted to the dimethylamides **3** and **4** by deprotonation with *n*-BuLi and quenching with dimethylcarbamoyl chloride (Scheme 1), and evaluated in a benchmark $HSiCl_3$ reduction of the *N*-PMP acetophenone ketimine **5** under a standard set of reaction conditions by removing aliquots and analyzing the conversion by ^1H NMR spectroscopy (Fig. 1). *N*,*N*-Dimethyl benzamide was included as a benchmark to compare the role of the imidazole nitrogen atom.

The data obtained show slightly different reactivities between the *N*-Me and *N*-*t*-Bu catalysts **1** and **2** but this may be

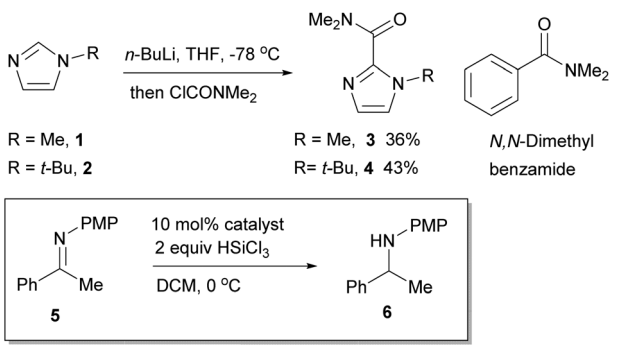

Scheme 1 Synthesis and evaluation of imidazole catalysts **1–4** and *N*,*N*-dimethyl benzamide.

Department of Chemistry, University of Sheffield, Dainton Building, Brook Hill, Sheffield, UK S3 7HF. E-mail: simon.jones@sheffield.ac.uk

†Electronic supplementary information (ESI) available: Copies of ^1H & ^{13}C NMR spectra, chromatographs and crystal structure of catalyst **17**. CCDC 1517809. For ESI and crystallographic data in CIF or other electronic format see DOI: 10.1039/c6ob02537d

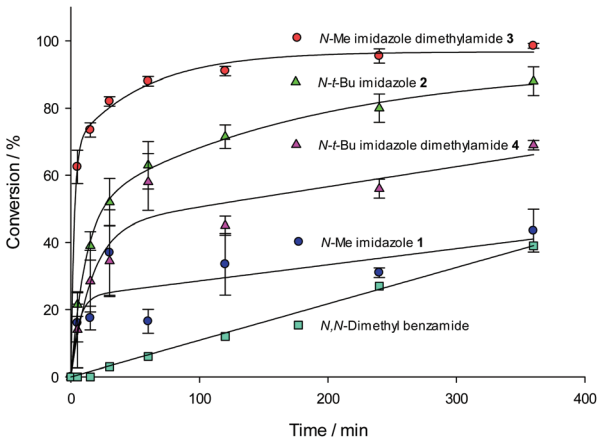

Fig. 1 Relative reaction rates of imidazole catalysts **1–4** and *N*,*N*-dimethyl benzamide. Reactions performed using 10 mol% catalyst, 2 equiv. $HSiCl_3$ in DCM (1 mL $mmol^{-1}$) at 0 °C. Conversion calculated from comparison of appropriate integrals in ^1H NMR spectrum of aliquots removed from reaction.

due to the *N*-Me catalyst not being completely soluble in DCM. However, what is noticeable is the significant difference in reaction rate between the two model dimethylamide catalysts; the *N*-Me catalyst **3** showed a significant increase in relative reaction rate compared to the parent imidazole, whilst the *N*-*t*-Bu catalyst **4** reaction rate dropped. This leads to the relative initial rate of the *N*-Me catalyst being of the order of 4 times faster than that of the *N*-*t*-Bu one. By comparison to the imidazole catalysts, *N*,*N*-dimethyl benzamide was a very poor catalyst, barely operating above the background reaction rate for these type of processes.

In order to probe this further, both dimethylamide catalysts **3** and **4** were studied using *in situ* infra-red experiments. The absorption signal of the carbonyl group of *N*-Me catalyst **3** in DCM initially appeared at 1635 cm^{-1} and after addition of one equivalent of $HSiCl_3$, a new signal immediately appeared at 1668 cm^{-1}, while the original signal at 1635 cm^{-1} simultaneously disappeared (Fig. 2). Addition of further equivalents of $HSiCl_3$ led to no additional change other a dilution effect (observed in the slight drop of the signal at 1668 cm^{-1} after 8 min). This suggests that coordination of $HSiCl_3$ with the amide is rapid and complete for this catalyst. In the case of the *N*-*t*-Bu catalyst **4**, the original signal of the carbonyl group was at 1645 cm^{-1} with a smaller new signal appearing at 1671 cm^{-1} once treated with one equivalent of $HSiCl_3$. Noticeably, in this case significant amounts of the uncoordinated catalyst were still present compared to the *N*-Me catalyst **3** and this ratio did not change with time, or when a further equivalent of $HSiCl_3$ was added. This suggests that coordination of this catalyst to $HSiCl_3$ is more difficult than in the case of the *N*-Me catalyst **3**, and that steric effects of the imidazole *N*-alkyl group play an important role in the activity of such catalysts. In complete contrast, *N*,*N*-dimethyl benzamide, showed no change in the carbonyl group signal, correlating with its poor reactivity.

For this series of compounds, it seems that the extent of coordination of the $HSiCl_3$ with the carbonyl group is a reasonable measure of catalytic activity. The *N*-Me and *N*-*t*-Bu catalysts are likely to incur different and significant energetic penalties for the interaction of the amide *N*-methyl groups with the imidazole alkyl substituent, in either case probably ruling out a truly co-planar species **7a** (Fig. 3). This probably favours a stable conformation that places the carbonyl group and imidazole ring orthogonal to each other *i.e.* structure **7b** in Fig. 3 (note that these are depicted as reactive conformations, not active catalytic species that might be protonated at the imidazole nitrogen atom, *vide infra*). The increasing torsional

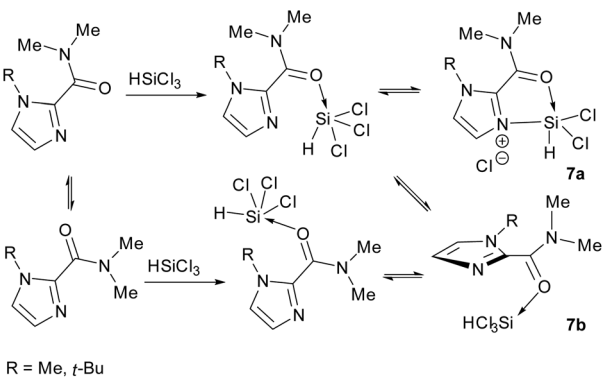

Fig. 3 Reactive conformations of catalysts **3** and **4**.

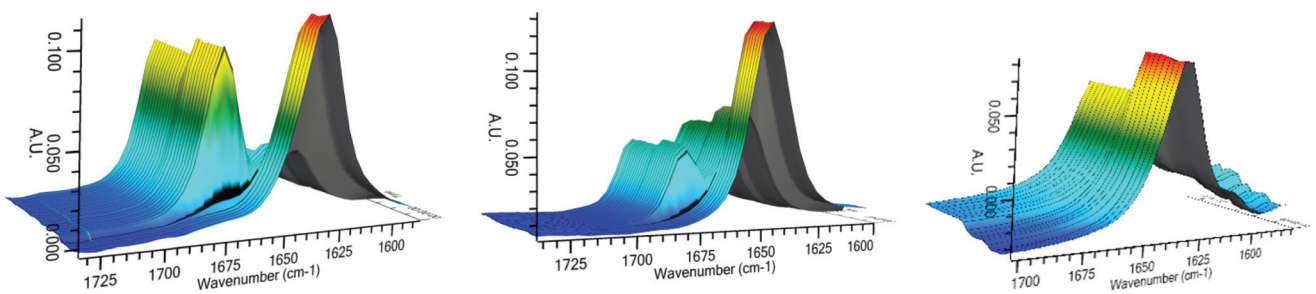

Fig. 2 From left to right; *in situ* IR data of *N*-Me catalyst **3** treated with $HSiCl_3$ as a function of time; *in situ* IR data of catalyst *N*-*t*-Bu **4** treated with $HSiCl_3$ as a function of time; *in situ* IR data of *N*,*N*-dimethyl benzamide treated with $HSiCl_3$ as a function of time.

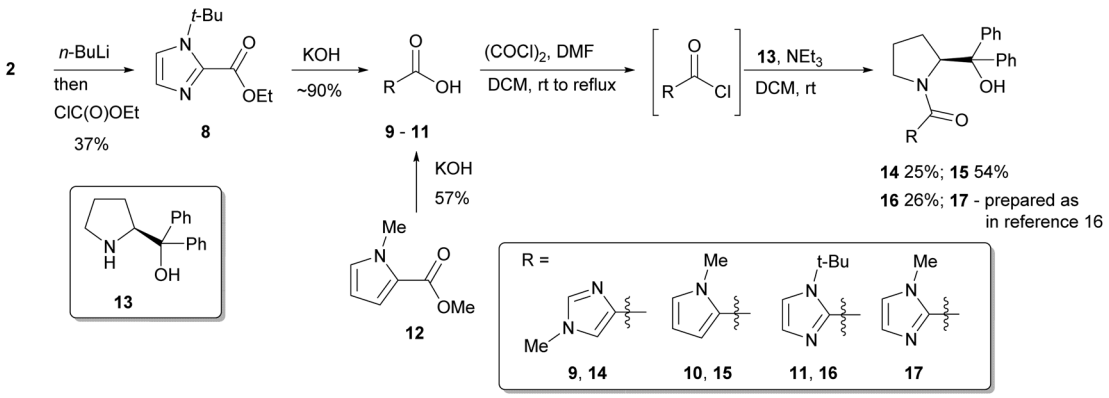

Scheme 2 Synthesis of catalysts **14–17**.

angle then in-turn increases the distance of the silicon and imidazole nitrogen atoms, reducing reactivity, fitting well with observations with the *N*,*N*-dimethyl benzamide system, that lacks any cooperative effect of the imidazole nitrogen atom.

Naturally, these catalyst fragments lack the prolinol moiety that might have synergistic effects when considering the whole catalyst system, and any speculation about mechanism for these simple amides might not directly translate to more complex systems. Thus, in order to further probe such interactions, a series of chiral heterocyclic catalysts were investigated containing a prolinol derived backbone that were prepared starting from their parent carboxylic acids. 1-Methylimidazole-4-carboxylic acid **9** is commercially available, and 1-methylpyrrole-2-carboxylic acid **10** was obtained by hydrolysis of the methyl ester **12** with aqueous potassium hydroxide. 1-*t*-Butylimidazole-4-carboxylic acid **11** was accessed by deprotonation of 1-*t*-butylimidazole **2** with *n*-BuLi then quenching with ethyl chloroformate to give the ester **8**, followed by basic hydrolysis. These three heterocyclic carboxylic acids **9–11** were transformed into the respective acid chlorides with oxalyl chloride, followed by immediate coupling with α,α-diphenylprolinol **13** giving catalysts **14–16**, with previously reported catalyst **17** being prepared by a similar method as previously described (Scheme 2).[16]

All of these new catalysts were then evaluated under the standard set of reaction conditions (Scheme 1 and Fig. 4). The isomeric imidazole **14** was active but led to poor selectivity delivering the opposite enantiomer of product amine **6** to that normally observed. Given the torsional freedom that this isomeric system has compared to the parent imidazole catalyst **17**, it is likely that an alternative reactive conformation may be accessible in this case, perhaps even a co-planar species analogous to **7a**, resulting in a competitive pathway with a different stereochemical bias. The *N*-Me pyrrole catalyst **15** was essentially inactive which is interesting as it indicates that the amide functionality alone is not sufficient to promote this reaction. Based on the kinetic data for the dimethylamide catalyst **4**, perhaps unsurprisingly the *N*-*t*-Bu catalyst **16** was essentially inactive, the 15% conversion being typical of the background reaction rate for this process. None of these surpassed the performance of the previously reported catalyst **17**. This compares well with the findings obtained with the simple, achiral catalysts **3** and **4**, whereby torsional freedom around the imidazole–carbonyl bond to appropriately locate the imidazole nitrogen atom is critical for high catalytic activity.

The previously reported development of the imidazole catalyst **17** clearly demonstrated some key requirements in order to obtain both high yields and selectivity.[16] Most critical for obtaining high selectivities was use of a *gem*-diaryl group. This most likely relays stereochemical information from the adjacent proline stereogenic center to create a chiral environment that facilitates the required facial differentiation of the planar ketimine.

In order to investigate this further, the *gem*-dimethyl catalyst **21** was prepared by coupling (*S*)-α,α-dimethylprolinol **19** (obtained from reaction of ester **18** with an excess of MeMgI, followed by hydrolysis) with ethyl *N*-methyl imidazole-1-carboxylate **20** and evaluated in the benchmark reduction of the *N*-PMP-ketimine of acetophenone **5** (Fig. 5 and Scheme 1). Noticeably, although the conversion to product was approximately the same as other catalysts previously prepared, the enantioselectivity was lower than that of the *gem*-diaryl catalyst **17**, and similar to the catalyst **22** without the *gem*-dimethyl group. Thus, the role of this component may not simply be

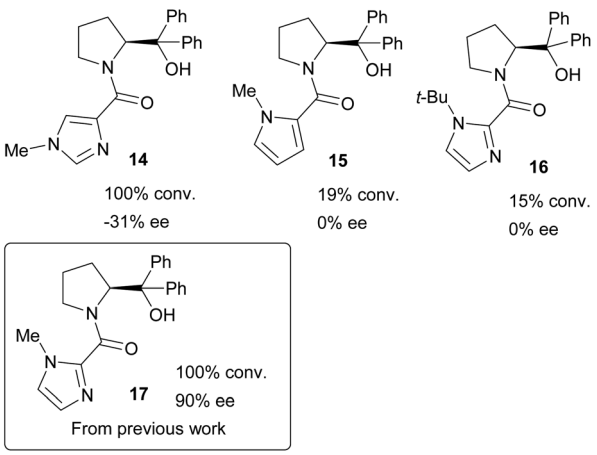

Fig. 4 Evaluation of prolinol catalysts **14–17** according to Scheme 1.

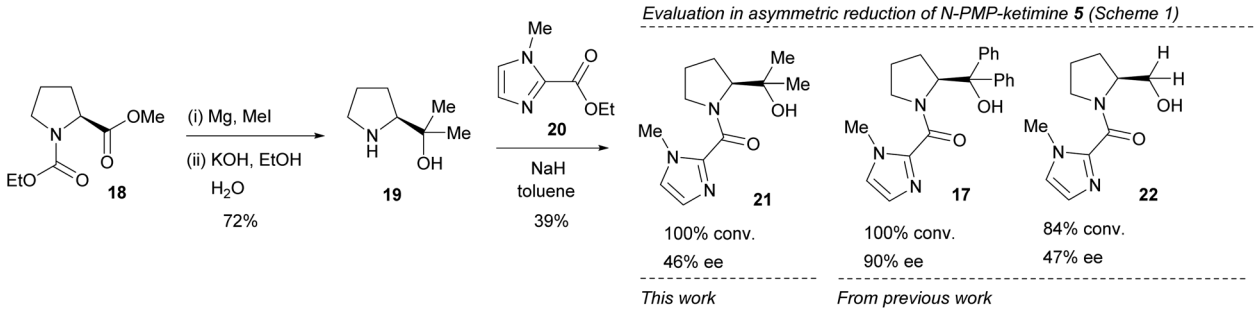

Fig. 5 Synthesis of catalyst **21** and comparison of activity with previous catalysts in the reduction of *N*-PMP ketimine **5** as shown in Scheme 1.

steric, an effect that has been previously documented for *gem*-diaryl groups.[21]

In the final stage of catalyst evaluation, the role of the hydroxyl group was examined. Matsumura's work had previously shown that the deoxy-picoline derivative **24** catalyzed the asymmetric hydrosilylation of *N*-phenyl ketimine **25** but led to poor selectivity compared to the parent catalyst **23**, inferring the need for a hydrogen bond to effectively coordinate with the ketimine substrate, leading to the commonly accepted model shown.[12] In order to compare this effect in the imidazole series, removal of the hydrogen bond acceptor was achieved by methylation of catalyst **17** with sodium hydride and methyl iodide giving the *O*-Me catalyst **26** in 56% yield (Scheme 3). For comparison purposes, Matsumura's picolinic acid derived catalyst **23** was prepared from commercially available 2-picolinic acid by treating with oxalyl chloride, then reaction with α,α-diphenylprolinol **13**. This was also *O*-methylated in analogous fashion to give catalyst **27** in 83% yield. These catalysts were then evaluated in the benchmark reduction of the *N*-PMP ketimine **5**, each being challenged at low catalyst loadings to better determine efficacy (Table 1). Commercially available Sigamide® **28** was also included to provide a frame of reference.

Imidazole derived catalyst **17** performed as expected, its reactivity dropping off slightly with reduced loading, but still acting in a reasonably stereoselective manner (Table 1, entries

Table 1 Evaluation of catalysts **17**, **23**, **26–28** according to the reaction shown in Scheme 1[a]

Entry	Catalyst	Catalyst loading (mol%)	Conversion[b] (%)	ee[c] (%)	ACE[d]
1	**17**	1	100	90	56
2		0.1	88	87	481
3		0.01	60	80	3018
4	**26**	1	100	91	58
5		0.1	100	89	538
6		0.01	96	84	4881
7	**23**	1	100	79	50
8	**27**	1	100	56	34
9		0.1	95	62	359
10		0.01	25	ND[e]	
11	**28**	1	60	80	31

[a] Reactions conducted with *N*-PMP-ketimine **5** (1 mmol), $HSiCl_3$ (2 mmol) at the specified catalyst loading in DCM (0.5 mL) at 0 °C for 4 h, followed by aqueous workup. [b] Conversion calculated by comparison of the value of the integrals for the product to residual ketimine and ketone (from hydrolysis). [c] Determined by chiral phase HPLC analysis. [d] See ref. 22. [e] Not determined.

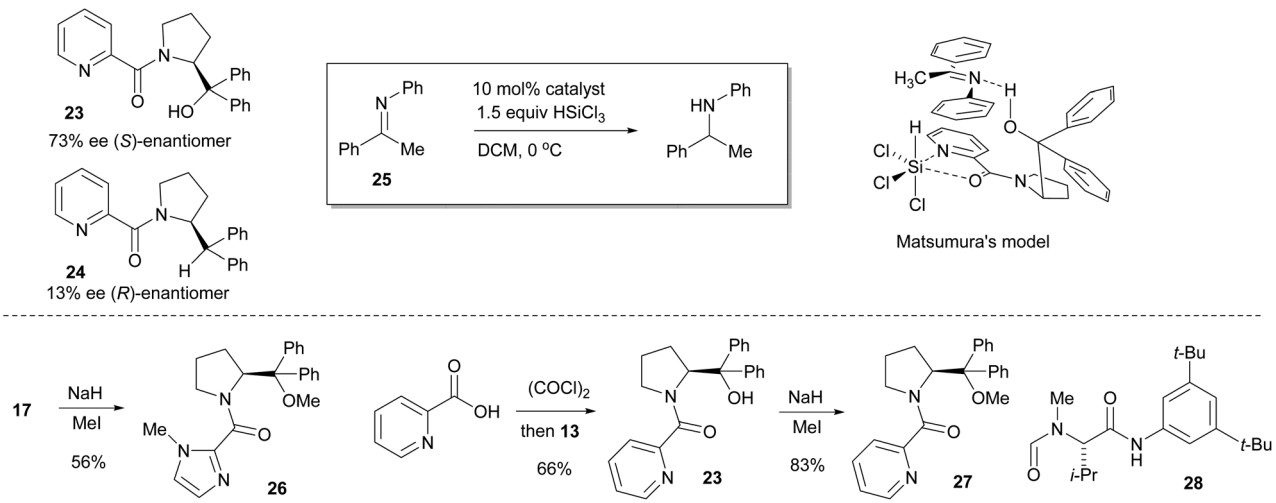

Scheme 3 Matsumura's picolinoyl catalysts **23** & **24** and selectivity model, synthesis of *O*-methyl catalysts **26** & **27**, and structure of Sigamide® **28**.

1–3). However, completely unexpectedly, methylated imidazole catalyst **26** showed superior activity and selectivity at even as low as 0.01 mol% loading (entries 4–6). Calculation and comparison of the Asymmetric Catalytic Efficiency (ACE)[22] factor at each of the catalyst loadings highlights the exceptional activity of methoxy catalyst **26** at low catalyst loading (Table 1, compare entries 3 and 6). Given the accepted hypothesis of the importance of the hydrogen bond, this is a remarkable and unprecedented result. Interestingly, a broadly similar trend was observed with the picoline catalysts **23** and **27** although not at the same performance level as the imidazole ones (entries 7–10). Under the conditions used, Sigamide® **28** did not perform as well as the other catalysts (entry 11).

The enhanced catalytic activity of catalyst **26** was exemplified with a small representative selection of ketimines **29–33**, with conversion and enantioselectivities of the product amines **34–38** comparable to those obtained at higher loading using catalyst **17** (Scheme 4 and Table 2). Given the structural similarity of these catalysts it is not surprising that the stereodifferentiating elements result in comparable selectivities and further exemplification and optimisation of reaction parameters was not carried out.

The remarkable and unexpected catalyst activity, presumably due to the absence of the hydrogen bond, warranted further investigation. The difference in hydroxy and methoxy catalysts **17** and **26** is first evident from their ^{1}H NMR spectra. Hydroxy catalyst **17** has a very broad and almost uninterpretable spectrum in $CDCl_3$ at room temperature and is best recorded in DMSO at 100 °C in order to obtain the best resolution signals, presumably due to the presence of an internal hydrogen bond, although this is not evident in the single crystal X-ray crystal structure (see ESI†). In contrast, methoxy catalyst **26** provides a much better resolved spectrum at room temperature in $CDCl_3$, existing as two rotameric forms in a 4.5 : 1 ratio.

In an attempt to elucidate the mechanism further, the relationship of product ee and catalyst ee was examined using the *N*-PMP-ketimine substrate **5** and hydroxy catalyst **17**. Plotting this gave a linear relationship (Fig. 6), indicating that one molecule of catalyst was involved in formation of the catalytically active species. Furthermore, the ee of the product remained constant over the duration of the experiment.

Since the critical unusual feature that was observed in this catalyst screen related to the hydroxyl group, further efforts were made to examine the chemistry around this centre by ^{1}H NMR and ^{29}Si NMR experiments. The reduction of *N*-PMP ketimine **5** was performed with $HSiCl_3$ (2 equiv.) in $CDCl_3$ with 1 mol% imidazole catalyst **17**.

After 4 h, ^{1}H NMR and ^{29}Si NMR spectroscopy indicated that the main species resulting from the reduction were *N*-$SiCl_2H$ amine **39** (δ_H 5.55 ppm and δ_{Si} −9.7 ppm) and silicon tetrachloride (δ_{Si} −18.9 ppm) (Fig. 7). The identity of the former species was confirmed by independent synthesis by addition of trichlorosilane to a sample of *N*-PMP-α-methylbenzylamine **6**, and the latter by comparison with a reference sample. It is noticeable that the silicon tetrachloride results from the reaction and is not present in the $HSiCl_3$.

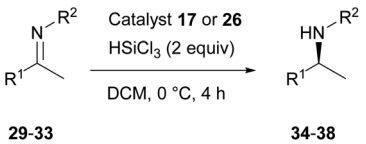

Scheme 4 Substrate scope with catalysts **17** and **26**.

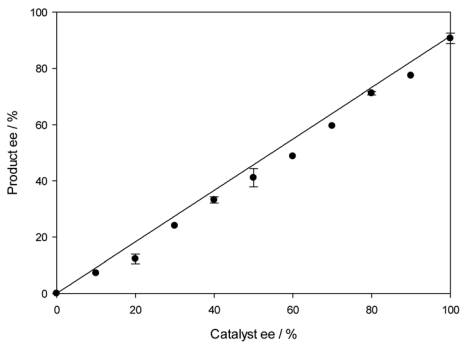

Fig. 6 Plot of product **5** ee *vs.* catalyst ee **17**.

Table 2 Substrate scope of catalysts **17** and **26** according to the reaction shown in Scheme 4[a]

Entry	Catalyst (loading per mol%)	R^1	R^2	Imine	Amine	Conversion[b] (%)	ee[c] (%)
1	**26** (0.1)	Ph	4-FC_6H_4	**29**	**34**	95	86
2	**17** (1)	Ph	4-FC_6H_4	**29**	**34**	96	87
3	**26** (0.1)	4-$MeOC_6H_4$	4-$MeOC_6H_4$	**30**	**35**	97	84
4	**17** (1)[d]	4-$MeOC_6H_4$	4-$MeOC_6H_4$	**30**	**35**	81	85
5	**26** (0.1)	4-$NO_2C_6H_4$	4-$MeOC_6H_4$	**31**	**36**	98	84
6	**17** (1)[d]	4-$NO_2C_6H_4$	4-$MeOC_6H_4$	**31**	**36**	85	86
7	**26** (0.1)	2-Thienyl	4-$MeOC_6H_4$	**32**	**37**	77	80
8	**17** (1)[e]	2-Thienyl	4-$MeOC_6H_4$	**32**	**37**	61	79
9	**26** (0.1)	β-Naphthyl	4-$MeOC_6H_4$	**33**	**38**	99	92
10	**17** (1)[d]	β-Naphthyl	4-$MeOC_6H_4$	**33**	**38**	86	86

[a] Reactions conducted with ketimine (1 mmol), $HSiCl_3$ (2 mmol) at the specified catalyst loading in DCM (0.5 mL) at 0 °C for 4 h, followed by aqueous workup. [b] Conversion calculated by comparison of the value of the integrals for the product to residual ketimine and ketone (from hydrolysis). [c] Determined by chiral phase HPLC analysis. [d] Literature values, see ref. 16. [e] Using reductive amination protocol, see ref. 17.

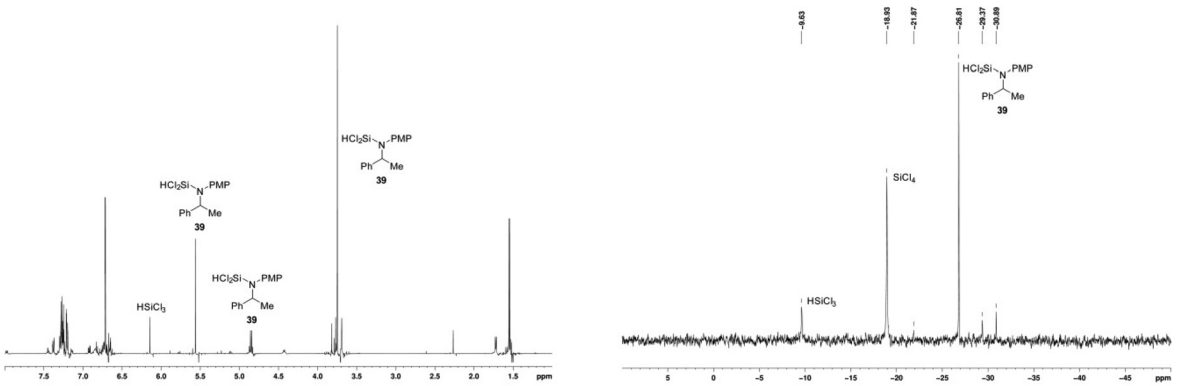

Fig. 7 *In situ* ^{1}H and ^{29}Si NMR spectra of reaction products as depicted in Scheme 1 with catalyst **17**.

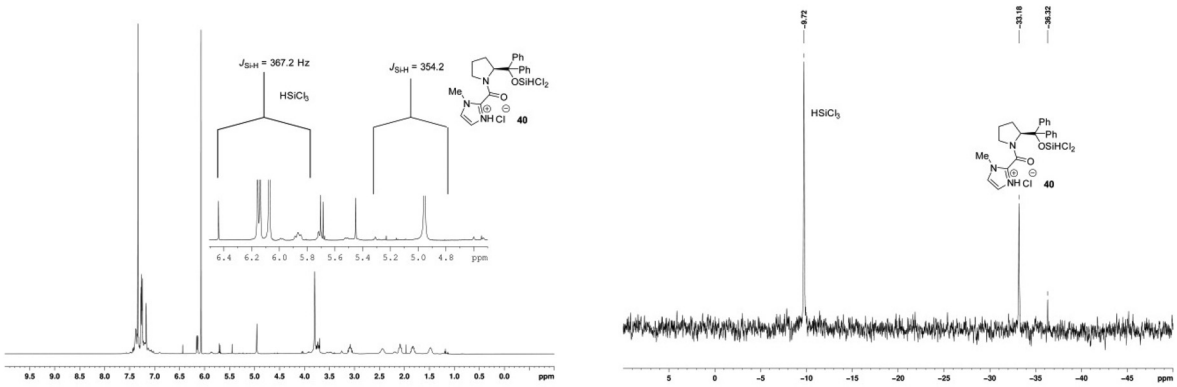

Fig. 8 ^{1}H and ^{29}Si NMR spectra of catalyst **17** and excess $HSiCl_3$.

When hydroxy catalyst **17** was treated with an excess of trichlorosilane, new signals were observed in the ^{1}H NMR (δ_H 4.99 ppm) and ^{29}Si NMR (δ_{Si} −33.2 ppm) spectra. These signals are consistent with an oxosilane species formed by silylating the hydroxyl group of catalyst **17**, confirmed by comparison of the ^{1}H and ^{29}Si chemical shifts of the related $EtOSiCl_2H$ in the literature, including J_{Si-H} coupling of ^{29}Si satellite signals in the ^{1}H NMR spectrum (Fig. 8).[23] Importantly, the ^{29}Si NMR spectrum only provided evidence for a tetra-coordinate silicon atom. The ^{1}H NMR spectrum also shows a significant downfield chemical shift of the methine proton adjacent to the amide nitrogen atom that might result as a combination of the loss of the internal hydrogen bond and from complexation of the carbonyl group to the silane. The spectrum also has considerably better resolved signals than that obtained for the parent catalyst at room temperature, implying fewer equilibrating rotameric and/or hydrogen bonded species. In retrospect, this is what one would expect from the natural reactivity of a chlorosilane with an alcohol to generate a silyl ether and HCl. Given the formation of the latter, it is also very likely that the imidazole of the catalyst will be protonated. Importantly, this preformed catalyst – trichlorosilane complex **40** demonstrated the same catalytic activity in the standard asymmetric hydrosilylation reaction, and returned unchanged catalyst after work-up. In contrast, no new signals were observed in the ^{29}Si NMR spectrum of the methoxy catalyst **26** when treated with trichlorosilane, which was corroborated by the presence of only a very small signal at δ_H 5.27 ppm in the ^{1}H NMR spectrum where evidence of a Si–H signal might be observed (Fig. 9). However, significant chemical shift changes were

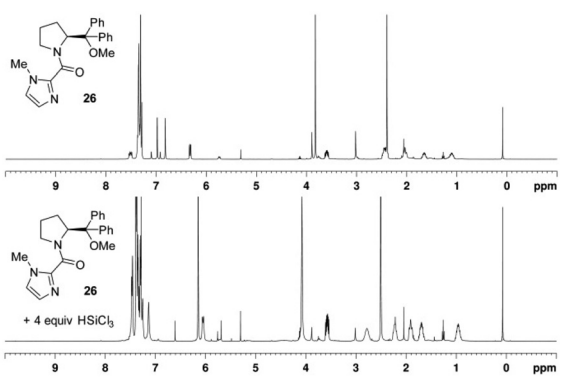

Fig. 9 ^{1}H NMR spectrum of catalyst **26** before and after addition of 4 equiv. $HSiCl_3$.

observed in the imidazole and methine protons, in addition to those signals corresponding to the pyrrolidine ring. As in the case of the hydroxyl-catalyst **17**, these changes may have resulted from protonation of the imidazole, in this case from adventitious HCl usually found in $HSiCl_3$.

The presence of HCl and protonation of the catalysts appeared to be a key factor in their activity, and related studies have also shown that additives such as water (to form HCl *in situ*), acetic acid, and benzoic acid can improve the catalytic activity.[6,7,9,24,25] As previously indicated, HCl is most likely also present in commercial $HSiCl_3$, and to confirm the effect of this, a series of reactions were performed under diluted conditions in order to slow them down sufficiently to observe positive or negative effects of the effects of proton sponge, HCl and chloride ions (in the form of *n*-BuN_4Cl). None of these additives catalysed the reaction in the absence of the catalysts, and reactions conducted with the hydroxy **17** and methoxy **26** catalysts showed that the presence of HCl was essential for reactivity (Table 3, entries 2 and 7).

As conducted with catalysts **3** and **4**, investigation of the reactive catalyst species was conducted by *in situ* infra-red analysis (Fig. 10 and 11). Upon addition of 1 equiv. of $HSiCl_3$, the hydroxy catalyst **17** shows a rapid and complete change in the stretching frequency of the carbonyl group, whilst catalyst **26** shows a rapid but incomplete change, suggesting an equilibrium process. This is very similar to the behaviour with the simpler catalysts **3** and **4**, however the reactivity is inverted, with catalyst **26** showing incomplete complexation being more active. Since no direct reaction with $HSiCl_3$ is possible here as corroborated by ^{29}Si NMR data, the changes in the ^{1}H NMR and IR data indicate a different resting state for the catalyst, perhaps with the imidazole being protonated by the small quantities of HCl present in the $HSiCl_3$. Catalyst **17** reacts stoichiometrically with $HSiCl_3$, in doing so generating HCl to completely protonate the imidazole.

Table 3 Effect of proton sponge, *n*-Bu_4NCl, and HCl on catalysts **17** and **26** according to reaction shown in Scheme 1[a]

Entry	Catalyst (loading per mol%)	Additive (equiv.)	Conversion[b]/%
1	**17** (0.1)	None	57
2	**17** (0.1)	Proton sponge (1)	0
3	**17** (0.1)	*n*-Bu_4NCl (0.1)	61
4	**17** (0.1)	HCl (0.005)	60
5	**17** (0.1)	HCl (0.05)	58
6	**26** (0.01)	None	13
7	**26** (0.01)	Proton sponge (1)	0
8	**26** (0.01)	*n*-Bu_4NCl (0.1)	15
9	**26** (0.01)	HCl (0.005)	15
10	**26** (0.01)	HCl (0.05)	16

[a] Reactions conducted with *N*-PMP-ketimine **5** (1 mmol), $HSiCl_3$ (2 mmol) with the specified additive and catalyst loading in DCM (5 mL) at 0 °C for 1 h, followed by aqueous workup. [b] Conversion calculated by comparison of the value of the integrals for the product to residual ketimine and ketone (from hydrolysis).

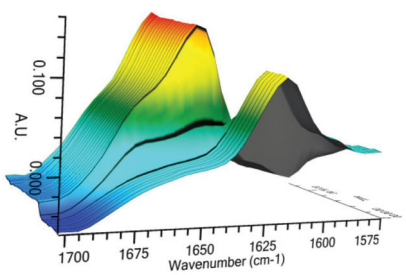

Fig. 10 *In situ* IR data of catalyst **17** treated with $HSiCl_3$ as a function of time.

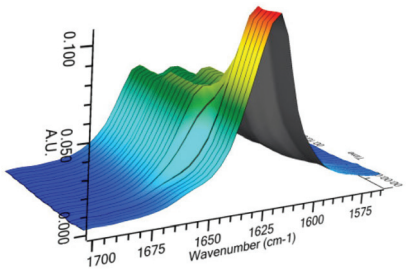

Fig. 11 *In situ* IR data of catalyst **26** treated with $HSiCl_3$ as a function of time.

Based on these results, a new 'dual activation' mechanistic model is proposed that involves a Lewis basic site to activate the $HSiCl_3$ and an additional Brønsted base capable of reacting with HCl generated or present in the reaction (Fig. 12). Reaction of the hydroxy catalyst **17** with $HSiCl_3$ provides a covalently linked siloxane **40** where the imidazole is protonated by HCl, either as a by-product from reaction with the alcohol, or from adventitious HCl in the $HSiCl_3$. This is the resting state for the catalyst that is set up for forming a key hydrogen bond with the ketimine substrate.

Coordination of the silane with the Lewis basic amide inferred from the *in situ* infra-red studies must involve twisting of the amide bond to negate steric interactions, leading to a reactive hexa-coordinate species **41**. The ketimine substrate is now activated by a hydrogen bond to the protonated imidazole, and placed in the correct orientation to facilitate hydride delivery from the activated siloxane. Importantly, the *N*-PMP-amine product **6** then undergoes reaction with more trichlorosilane to generate the observed *N*-$SiHCl_2$ product **39**, whilst the inactive catalyst **42** turns-over by protonation and reaction with more trichlorosilane, generating silicon tetrachloride. This accounts for the observation that the reaction slows considerably when using less than 2 equivalents of $HSiCl_3$.

This model essentially inverts that proposed by Matsumura (Scheme 3), with the crucial hydrogen bond now being located at the imidazole nitrogen atom. However, the deoxy catalyst **23** may still react *via* the previously accepted model, especially as there is some similarity between the sense and magnitude of the selectivity observed with catalyst **14** (Fig. 4).

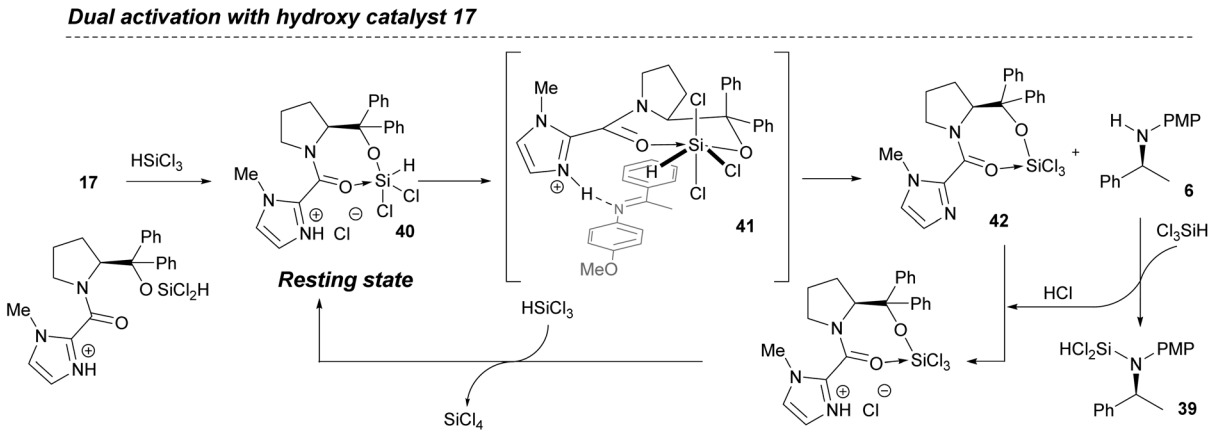

Fig. 12 Proposed dual activation mechanism for catalyst **17**.

The process with methoxy catalyst **26** is more complex since no evidence could be obtained for a species whereby $HSiCl_3$ is bound to the catalyst. Clearly there is a change in the ^1H NMR and IR data on addition of $HSiCl_3$ that may be due to reaction with HCl (Fig. 13). Naturally this means that no Si–O bond needs to be broken after reduction of the C=N bond and therefore the catalyst can turn-over more quickly, perhaps explaining the enhanced catalytic activity. A completely different mechanism is unlikely due to the similar levels of enantioselectivity that catalysts **17** and **26** provide.

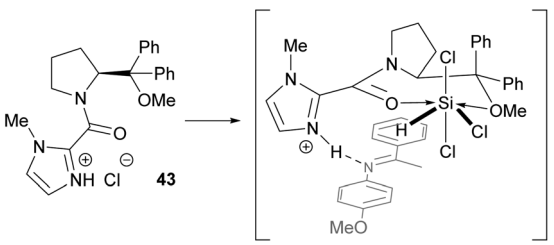

Fig. 13 Postulated resting state **43** and intermediate in dual activation mechanism with methoxy catalyst **26**.

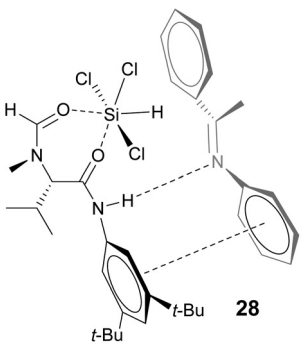

Fig. 14 Previously reported model for Sigamide **28** illustrating dual activation.

Such a dual activation model is obviously transferable to the Matsumura and related picoline systems, the difference in reactivity probably now coming from the different torsional freedom and basicity provided by the 2-pyridyl moiety. The model previously proposed for related *N*-formamide catalysts such as Sigamide® **28** also contains key elements of this dual activation mechanism, with the Brønsted acid now being the relatively acidic aniline NH proton (Fig. 14).

Conclusion

In summary, a dual-activation mechanism is proposed for the organocatalyzed asymmetric hydrosilylation of ketimines. This model fits the available mechanistic and characterization data and in doing so has provided an example of a new catalyst system displaying catalytic activity at unprecedented low levels of catalyst loading. Computational studies on these systems may reveal more details to support these studies. This work should provide valuable insights for the future design and mechanistic rationale for new catalysts in this area.

Experimental section

General experimental methods

All solvents were obtained from a dry solvent system and glassware was flame dried and cooled under vacuum before use. All dry reactions were carried out under a nitrogen atmosphere. TLC was carried out using aluminium TLC sheets (silica gel 60 F_{254}), and visualised using a UV lamp or by dipping in $KMnO_4$ solution then exposure to heat. Flash column chromatography was carried out with silica gel 40–63 μ 60 Å. ^1H, ^{13}C NMR and ^{29}Si spectra were measured using $CDCl_3$ as solvent unless otherwise stated. ^{13}C NMR spectra were recorded using the JMOD method. Specific rotations were measured at 589 nm (Na D-Line) at 20 °C unless otherwise stated, and are given in 10^{-1} deg cm^2 g^{-1}. All chemicals were used as received without further purification. Previously reported methods were used to

prepare the following compounds: *N*-PMP-ketimine **5**, (*S*)-α,α-diphenylprolinol **13**, *N*-Me-catalyst **17**, (*S*)-*N*-ethoxycarbonyl-proline methyl ester **18**, ethyl *N*-methyl imidazole-1-carboxylate **20**, 4-methoxy-*N*-[1-(4-nitrophenyl)ethylidene]benzenamine **31**, 4-methoxy-*N*-[1-(2-naphthalenyl)ethylidene]benzenamine **33**;[16] 4-fluoro-*N*-(1-phenylethylidene)benzenamine **29**, 4-methoxy-*N*-[1-(4-methoxyphenyl)ethylidene]benzenamine **30**;[26] *N*-4-methoxy-*N*-[1-(2-thienyl)ethylidene]benzenamine **32**.[19]

1-*t*-Butylimidazole 2

The title compound was prepared using a modified literature procedure.[20] A 250 mL three-necked flask containing distilled water (50 mL) was equipped with two dropping funnels and a condenser. One dropping funnel was filled with a mixture of 40% aqueous glyoxal (11.5 mL, 0.1 mol) and 37% aqueous formaldehyde (8.10 g, 0.1 mol), the other with *t*-butylamine (10.6 mL, 0.1 mol) and 35% aqueous ammonia (4.86 g, 0.1 mol). The water was heated until boiling, and then both solutions were added simultaneously at the same addition rate. The resulting mixture turned brown and was stirred for 30 min at reflux after complete addition, and then cooled to rt. The mixture was extracted with DCM (3 × 150 mL), the combined organic phases were washed with brine (50 mL) and dried over $MgSO_4$. The desiccant was filtered off and the filtrate was evaporated. The brown residue was purified by vacuum distillation to give the product **2** as a colourless oil (4.80 g, 39%); δ_H (400 MHz, $CDCl_3$): 1.55 [9H, s, $(CH_3)_3C$], 7.03 (1H, s, ArC*H*), 7.04 (1H, s, ArC*H*), 7.60 (1H, s, ArC*H*); δ_C (100 MHz, $CDCl_3$): 30.6 [$C(CH_3)_3$], 54.7 [$C(CH_3)_3$], 116.3 (Ar*C*H), 129.1 (Ar*C*H), 134.3 (Ar*C*H); Data were in accordance with the literature.

1-Methyl-*N*,*N*-dimethyl-1*H*-imidazole-2-carboxamide 3[27]

N-Methylimidazole **1** (1.64 g, 20 mmol) was dissolved in THF (20 mL) and cooled to −78 °C. *n*-BuLi (2.5 M in hexanes, 10 mL, 25 mmol) was added dropwise by syringe. The resulting mixture was stirred at −78 °C for 2 h. This solution was added dropwise to a solution of dimethylcarbamoyl chloride (2.99 g, 28 mmol) in diethyl ether (25 mL) at −78 °C and stirred for 1 h at the same temperature. The reaction mixture was then warmed to rt and quenched with water (50 mL). The organic solvent was evaporated and the aqueous was extracted with DCM (3 × 30 mL) and dried over $MgSO_4$. The desiccant was filtered off and the filtrate was evaporated to give the crude residue, which was purified by chromatography on silica gel [50%–100% ethyl acetate in petroleum ether (40–60)] to yield the product **3** as a colourless oil (1.10 g, 36%); δ_H (400 MHz, $CDCl_3$): 3.12 (3H, s, CH_3), 3.41 (3H, s, CH_3), 3.89 (3H, s, CH_3), 6.94 (1H, d, *J* 1.0, ArC*H*), 7.05 (1H, d, *J* 1.0, ArC*H*); δ_C (100 MHz, $CDCl_3$): 35.0 (CH_3), 35.7 (CH_3), 39.3 (CH_3), 123.6 (Ar*C*H), 127.3 (Ar*C*H), 140.1 (Ar*C*), 160.9 (*C*O); Data was in accordance with the literature.

1-*t*-Butyl-*N*,*N*-dimethyl-1*H*-imidazole-2-carboxamide 4

1-*t*-Butylimidazole **2** (2.48 g, 20 mmol) was dissolved in THF (20 mL) and cooled to −78 °C. *n*-BuLi (2.0 M in hexanes, 12.5 mL, 25 mmol) was added dropwise by syringe. The resulting mixture was stirred at −78 °C for 2 h. This solution was added dropwise to a solution of dimethylcarbamoyl chloride (2.99 g, 28 mmol) in diethyl ether (20 mL) at −78 °C and stirred for 1 h at the same temperature. The reaction mixture was then warmed to rt and quenched with water (50 mL). The organic solvent was evaporated and the aqueous was extracted with DCM (3 × 100 mL) and dried over $MgSO_4$. The desiccant was filtered off and the filtrate was evaporated to give the crude residue. Pure product 4 was obtained as a white solid after recrystallization from ethyl acetate (1.69 g, 43%); m.p. 146–148 °C; ν_{max} (thin film): 3157 (w), 2931 (w), 1638 (s), 1524 (w); δ_H (400 MHz, $CDCl_3$): 1.60 [9H, s, $(CH_3)_3C$], 2.96 (3H, s, CH_3), 3.09 (3H, s, CH_3), 6.97 (1H, d, *J* 1.2, ArC*H*), 7.05 (1H, d, *J* 1.2, ArC*H*); δ_C (100 MHz, $CDCl_3$): 30.4 (CH_3), 35.0 (CH_3), 38.6 (CH_3), 57.0 [$(CH_3)_2C$], 117.9 (Ar*C*H), 126.8 (Ar*C*H), 140.3 (Ar*C*), 164.5 (*C*O); HRMS (ES^+ TOF): found 196.1442 ($[M + H]^+$); $C_{10}H_{18}N_3O$ requires 196.1450.

Kinetic analysis of the reduction of ketimine 5 to amine 6

N-PMP-ketimine **5** (0.225 g, 1.0 mmol) and catalyst (mol% as specified) were dissolved in DCM (1 mL) at 0 °C. $HSiCl_3$ (0.2 mL, 2.0 mmoL) was added and the reaction left to stir for the specified time. Work-up, either after the reaction was complete, or by removal of samples during the reaction, was accomplished by dilution with DCM (20 mL per mL aliquot), quenching with aqueous NaOH (1 M, approximately 20 mL per mL aliquot), and separation of the organic layer. The aqueous layer was further extracted with DCM (2 × 20 mL per mL aliquot), the combined organic layers dried over $MgSO_4$, filtered and evaporated. Conversion was calculated from comparison of the integrals corresponding to ketimine starting material(s) and ketone (from hydrolysis of the ketimine) and that of the product amine **6**. δ_H (400 MHz, $CDCl_3$): 1.52 (3H, d, *J* 7.1, CH_3), 3.70 (3H, s, CH_3), 4.43 (1H, q, *J* 7.1, C*H*), 6.49 [2H, $(AX)_2$, ArC*H*], 6.72 [2H, $(AX)_2$, ArC*H*], 7.21–7.40 (5H, m, ArC*H*).

Ethyl 1-*t*-butyl-1*H*-imidazole-2-carboxylate 8

1-*t*-Butylimidazole **2** (4.34 g, 35 mmol) was dissolved in THF (30 mL) and cooled to −78 °C. *n*-BuLi (2 M in hexanes, 20 mL, 40 mmol) was added dropwise by syringe. The resulting mixture was stirred at −78 °C for 2 h, and this solution added to a solution of ethyl chloroformate (7.56 g, 70 mmol) in THF (20 mL) by cannula at −78 °C, followed by stirring for 1 h at the same temperature. The reaction mixture was then warmed to rt and quenched with saturated aqueous ammonium chloride (50 mL). The resulting mixture was extracted with ethyl acetate (4 × 100 mL), and the combined organic layers were washed with brine (100 mL) and dried over $MgSO_4$. The desiccant was filtered off and the filtrate was evaporated. The residue was purified by chromatography on silica gel [(20%–30%) ethyl acetate in petroleum ether (40–60)] to yield the product **8** as a colourless oil (2.50 g, 37%); ν_{max} (thin film) 2980 (m), 1721 (s), 1403 (m); δ_H (400 MHz, $CDCl_3$): 1.41 (3H, t, *J* 7.1, CH_3), 1.50 [9H, s, $(CH_3)_3$], 4.38 (2H, q, *J* 7.1, CH_2),

7.06 (1H, s, ArC*H*), 7.23 (1H, s, ArC*H*); δ_C (100 MHz, $CDCl_3$): 14.2 (*C*H_3), 30.1 [(*C*H_3)$_3$], 58.7 [(CH_3)$_3$*C*], 61.6 (*C*H_2), 122.2 (Ar*C*H), 127.8 (Ar*C*H), 137.4 (Ar*C*), 160.0 (*C*O); HRMS (ES^+ TOF): found 197.1299 ($[M + H]^+$); $C_{10}H_{17}N_2O_2$ requires 197.1290.

1-Methyl-2-pyrrolecarboxylic acid 10

Aqueous KOH (2.5 M, 20 mL, 50 mmol) was added to a solution of methyl 1-methylpyrrole-2-carboxylate **12** (2.1 g, 6.6 mmol) dissolved in methanol (20 mL) at rt and the resulting reaction mixture was stirred overnight. Methanol was evaporated and the remaining solution was carefully acidified to pH 2 with hydrochloric acid (6 M). The white precipitate was collected by filtration and washed with water. The precipitate was dissolved in DCM (50 mL) and dried over $MgSO_4$. The desiccant was filtered off and the filtrate was evaporated to give the product **10** as a white solid (1.1 g, 57%); m.p. 136–138 °C (lit.[28] 135–136 °C); δ_H (400 MHz, $CDCl_3$): 3.96 (3H, s, CH_3), 6.18 (1H, dd, *J* 4.0, 2.1, ArC*H*), 6.87 (1H, t, *J* 2.1, ArC*H*), 7.13 (1H, dd, *J* 4.0, 2.1, ArC*H*), 12.20 (1H, br s, O*H*); δ_C (63 MHz, $CDCl_3$): 37.0 (*C*H_3), 108.4 (Ar*C*H), 120.1 (Ar*C*H), 121.8 (Ar*C*), 130.8 (Ar*C*H), 166.6 (*C*O). NMR data was not previously reported in the literature.

1-*t*-Butyl-1*H*-imidazole-2-carboxylic acid 11

Aqueous KOH (2.5 M, 20 mL, 50 mmol) was added to a solution of ethyl 1-*t*-butyl-1*H*-imidazole-2-carboxylate **8** (1.29 g, 6.6 mmol) in methanol (20 mL) at rt. The reaction mixture was stirred overnight, the methanol was evaporated and the mixture carefully acidified to pH 2 with concd. HCl. The resulting mixture was evaporated to give a white solid that was treated with methanol (30 mL) and filtered. The filtrate was evaporated to give the crude product **11** as a white solid (0.70 g) that was contaminated with a small amount of the *t*-butyl imidazole compound formed by decarboxylation (~10%) but was used in the next step without further purification; δ_H (400 MHz, MeOD): 1.86 [9H, s, (*C*H_3)$_3$C], 7.71 (1H, d, *J* 1.8, ArC*H*), 8.02 (1H, d, *J* 1.8, ArC*H*); δ_C (100 MHz, MeOD): 28.3 [(*C*H_3)$_3$], 63.9 [(CH_3)$_3$*C*], 119.1 (Ar*C*H), 124.3 (Ar*C*H), 134.8 (Ar*C*), 154.8 (*C*O); HRMS (ES^+ TOF): found 169.0978 $[M + H]^+$; $C_8H_{13}N_2O_2$ requires 169.0977; Data for the *N*-*t*-butylimidazole contaminant; δ_H (400 MHz, MeOD): 1.72 [9H, s, (*C*H_3)$_3$], 7.63 (1H, s, ArC*H*), 7.91 (1H, s, ArC*H*), 9.10 (1H, s, ArC*H*).

(*S*)-[2-(Hydroxydiphenylmethyl)pyrrolidin-1-yl](1-methyl-1*H*-imidazol-4-yl)methanone 14

Oxalyl chloride (0.18 mL, 2.1 mmol) was added to a mixture of 1-methyl-1*H*-imidazole-4-carboxylic acid **9** (132 mg, 1.05 mmol) in DCM (5 mL) at rt. One drop of DMF was added and the reaction mixture was stirred at room temperature for 2 h. Excess oxalyl chloride and DCM were removed by evaporation under reduced pressure. The residue was dissolved in DCM (5 mL) and added to a solution of amino alcohol **13** (253 mg, 1.0 mmol) and triethylamine (0.2 mL, 1.4 mmol) in DCM (5 mL). The resulting mixture was stirred at rt for 2 h and then quenched with aqueous saturated $NaHCO_3$ (15 mL). The aqueous phase was extracted with DCM (3 × 15 mL), and the combined organic extracts washed with brine (15 mL) and dried over $MgSO_4$. The desiccant was filtered off and the filtrate was evaporated. The residue was purified by chromatography on silica gel (diethyl ether to flush off excess amino alcohol then 2% methanol in ethyl acetate) to yield the product **14** as a white solid (91 mg, 25%); m.p. 68–70 °C; $[\alpha]_D^{20}$ −116.3 (*c* 0.94, $CHCl_3$); ν_{max} (thin film) 2924 (s), 2854 (m), 1587 (m), 1556 (m), 1446 (m), 1434 (m); δ_H (500 MHz, 100 °C, DMSO-d_6): 1.30–1.39 (1H, m, C*H*H), 1.51–1.60 (1H, m, C*H*H), 1.88–1.94 (1H, m, C*H*H), 1.99–2.07 (1H, m, C*H*H), 3.28–3.34 (1H, m, C*H*H), 3.63 (3H, s, CH_3), 4.08–4.13 (1H, m, C*H*H), 5.67 (1H, br s, C*H*), 6.63 (1H, s, ArC*H*), 7.15–7.20 (3H, m, ArC*H*), 7.22–7.25 (1H, m, ArC*H*), 7.28–7.36 (5H, m, ArC*H*), 7.43–7.45 (2H, m, ArC*H*), 7.50 (1H, s, ArC*H*); δ_C (126 MHz, 100 °C, DMSO-d_6): 22.4 (*C*H_2), 27.6 (*C*H_2), 32.4 (*C*H_3), 48.3 (*C*H_2), 64.3 (*C*H), 80.8 (*C*), 125.1 (Ar*C*H), 125.7 (Ar*C*H), 126.0 (Ar*C*H), 126.5 (2 × Ar*C*H), 126.7 (2 × Ar*C*H), 126.8 (2 × Ar*C*H), 127.1 (2 × Ar*C*H), 136.4 (Ar*C*H), 136.9 (Ar*C*), 144.6 (Ar*C*), 146.1 (Ar*C*), 163.6 (CO); HRMS (ES^+ TOF): found 362.1876 $[M + H]^+$; $C_{22}H_{24}N_3O_2$ requires 362.1869.

(*S*)-[2-(Hydroxydiphenylmethyl)pyrrolidin-1-yl](1-methyl-1*H*-pyrrol-2-yl)methanone 15

Oxalyl chloride (0.18 mL, 2.1 mmol) was added to a solution of 1-methyl-2-pyrrolecarboxylic acid **10** (131 mg, 1.05 mmol) in DCM (5 mL) at room temperature. One drop of DMF was added and then the reaction mixture was stirred at rt for 2 h. Excess oxalyl chloride and DCM were removed by evaporation under reduced pressure. The residue was dissolved in DCM (5 mL) and added to a solution of amino alcohol **13** (253 mg, 1 mmol) and triethylamine (0.2 mL, 1.4 mmol) in DCM (5 mL). The resulting mixture was stirred at rt for 2 h and then quenched with aqueous saturated $NaHCO_3$ (15 mL). The aqueous phase was extracted with DCM (3 × 15 mL), and the combined organic extracts washed with brine (15 mL) and dried over $MgSO_4$. The desiccant was filtered off, the filtrate evaporated, and the residue purified by chromatography on silica gel [15% ethyl acetate in petroleum ether (40–60)] to yield the product **15** as a white solid (195 mg, 54%); m.p. 184–186 °C; $[\alpha]_D^{20}$ −83.7 (*c* 0.86, $CHCl_3$); (Found: C, 76.28; H, 6.64; N, 7.69. $C_{23}H_{24}N_2O_2$ requires C, 76.64; H, 6.71; N, 7.77%); ν_{max} (thin film) 3246 (w), 2958 (w), 1588 (s), 1435 (s); δ_H (400 MHz, $CDCl_3$): 1.42 (1H, pent d, *J* 7.5, 4.1, C*H*H), 1.61 (1H, d pent, *J* 12.4, 8.8, C*H*H), 1.94–2.03 (1H, m, C*H*H), 2.18 (1H, dtd, *J* 12.4, 8.8, 4.1, C*H*H), 2.92 (1H, td, *J* 10.0, 7.3, C*H*H), 3.76–3.79 (1H, m, C*H*), 3.81 (3H, s, CH_3), 5.50 (1H, dd, *J* 8.4, 7.4, C*H*), 6.08 (1H, dd, *J* 3.9, 2.0, ArC*H*), 6.23 (1H, dd, *J* 3.9, 2.0, ArC*H*), 6.70 (1H, app t, *J* 2.0, ArC*H*), 6.75 (1H, br s, O*H*), 7.27–7.39 (6H, m, ArC*H*), 7.48–7.50 (2H, m, ArC*H*), 7.55–7.58 (2H, m, ArC*H*); δ_C (100 MHz, $CDCl_3$): 24.5 (*C*H_2), 29.3 (*C*H_2), 36.3 (*C*H_3), 51.6 (*C*H_2), 66.8 (*C*H), 82.7 (*C*), 107.1 (Ar*C*H), 114.6 (Ar*C*H), 125.5 (Ar*C*), 127.1 (Ar*C*H), 127.2 (Ar*C*H), 127.3 (Ar*C*H), 127.4 (2 × Ar*C*H), 127.9 (2 × Ar*C*H), 128.0 (2 × Ar*C*H), 128.2 (2 × Ar*C*H), 143.1 (Ar*C*), 145.7 (Ar*C*), 165.5 (*C*O); HRMS (ES^+ TOF): found 361.1913 $[M + H]^+$; $C_{23}H_{25}N_2O_2$ requires 361.1916.

(*S*)-(1-*t*-Butyl-1*H*-imidazol-2-yl)[2-(hydroxydiphenylmethyl) pyrrolidin-1-yl]methanone 16

Oxalyl chloride (0.18 mL, 2.1 mmol) was added to the crude mixture of 1-*t*-butyl-1*H*-imidazole-2-carboxylic acid **11** (0.133 mg, 1.05 mmol) in DCM (5 mL) at room temperature. One drop of DMF was added and then the reaction mixture was stirred at rt for 2 h. The excess oxalyl chloride and DCM were removed by evaporation under reduced pressure. The residue was dissolved in DCM (5 mL) and this added to a solution of amino alcohol **13** (253 mg, 1 mmol) and triethylamine (0.2 mL, 1.4 mmol) in DCM (5 mL). The resulting mixture was stirred at rt for 2 h and then quenched with aqueous saturated $NaHCO_3$ (15 mL). The aqueous phase was extracted with DCM (3 × 15 mL), and the combined organic extracts washed with brine (15 mL) and dried over $MgSO_4$. Filtration and evaporation was followed by purification by chromatography on silica gel [diethyl ether to flush off excess amino alcohol, then 50% ethyl acetate in petroleum ether (40–60)] yielding the product **16** as a white solid (110 mg, 26%); m.p. 157–159 °C; $[\alpha]_D^{20}$ −153.7 (*c* 0.8, $CHCl_3$); ν_{max} (thin film) 2979 (w), 1618 (s), 1449 (s); δ_H (500 MHz, 100 °C, DMSO-d_6): 1.40 (1H, br s, C*H*H), 1.45 [9H, s, $(CH_3)_3$], 1.53–1.62 (1H, m, C*H*H), 1.93–1.99 (1H, m, C*H*H), 2.01–2.08 (1H, m, C*H*H), 3.19–3.24 (1H, m, C*H*H), 3.46 (1H, br s, C*H*H), 5.41 (1H, dd, *J* 8.3, 3.3, C*H*), 6.22 (1H, br s, ArC*H*), 6.86 (1H, s, ArC*H*), 7.13–7.16 (1H, m, ArC*H*), 7.20–7.25 (4H, m, ArC*H*), 7.29–7.32 (2H, m, ArC*H*), 7.42 (2H, d, *J* 7.5, ArC*H*), 7.48 (2H, d, *J* 7.7, ArC*H*); δ_C (126 MHz, 100 °C, DMSO-d_6): 22.2 (CH_2), 27.6 (CH_2), 29.5 [$(CH_3)_3C$], 48.6 [$(CH_3)_3C$], 56.4 (CH_2), 64.5 (*C*H), 80.4 (*C*), 118.4 (Ar*C*H), 125.4 (Ar*C*H), 125.8 (Ar*C*H), 126.1 (Ar*C*H), 126.6 (2 × Ar*C*H), 126.7 (2 × Ar*C*H), 126.9 (Ar*C*H), 140.4 (Ar*C*), 144.9 (Ar*C*), 145.8 (Ar*C*), 163.7 (*C*O); HRMS (ES^+ TOF): found 404.2348 $[M + H]^+$; $C_{25}H_{30}N_3O_2$ requires 404.2338.

General procedure A for the reduction of ketimines with catalysts

Ketimine (1.0 mmol) and catalyst (mol% as specified) were dissolved in DCM (1 mL) at 0 °C. $HSiCl_3$ (0.2 mL, 2.0 mmoL) was added and the reaction left to stir for the specified time. The reaction was quenched with aqueous HCl (1 M, 2 mL – care, gas evolution), followed by addition of DCM (20 mL) and aqueous NaOH (1 M, 20 mL), and stirred until the precipitate dissolved. The organic layer was separated and the aqueous layer was further extracted with DCM (2 × 20 mL). The combined organic layers were dried over $MgSO_4$, filtered and evaporated. Purification and analysis is detailed in individual amine products.

Catalyst evaluation using (*S*)-*N*-(4-methoxyphenyl)-α-methylbenzenemethanamine 6

Prepared by general procedure A, using 4-methoxy-*N*-(1-phenylethylidene)-benzenamine **5** (225 mg, 1 mmol) and specified catalyst, gave the title compound **6**. Conversion to product was determined by comparison of the integrals of signals in the ^1H NMR spectrum, whilst the enantiomeric excess was determined by chiral phase HPLC analysis; δ_H (400 MHz, $CDCl_3$): 1.52 (3H, d, *J* 7.1, CH_3), 3.70 (3H, s, CH_3), 4.43 (1H, q, *J* 7.1, C*H*), 6.49 [2H, $(AX)_2$, ArC*H*], 6.72 [2H, $(AX)_2$, ArC*H*], 7.21–7.40 (5H, m, ArC*H*); Phenomenex Lux 3 μm cellulose-1, hexane/i-PrOH = 98/2, flow rate = 1.0 mL min^{-1}, 254 nm, (*R*) enantiomer t_R = 16.5 min, (*S*) enantiomer t_R = 19.3 min.

(*S*)-α,α-Dimethyl-2-pyrrolinol 19[29]

Mg (1.92 g, 80 mmol), iodine (one granule) and diethyl ether (20 mL) were added to a dry three-necked flask. A solution of MeI (4.98 g, 80 mmol) in diethyl ether (80 mL) was added dropwise (initiated by heat after about 5–10 mL addition). The mixture was stirred at rt for 2 h and then cooled to 0 °C. A solution of (*S*)-*N*-ethoxycarbonylproline methyl ester **18** (4.02 g, 20 mmol) in diethyl ether (20 mL) was added dropwise. The resulting mixture was stirred at rt overnight, cooled to 0 °C and quenched with saturated aqueous ammonium chloride (50 mL). The organic layer was separated and the aqueous layer extracted with diethyl ether (2 × 50 mL). The combined organic extracts were evaporated to afford a yellow oil (3.36 g). This residue was treated with KOH (9.3 g, 0.166 mol), water (60 mL) and ethanol (40 mL), and heated at reflux overnight. The mixture was cooled to rt and the ethanol removed under reduced pressure. The resulting solution was extracted with DCM (2 × 50 mL), the combined extracts were washed with brine (30 mL) and dried over $MgSO_4$. After filtration, the filtrate was evaporated under reduced pressure to afford the title compound **19** as a brown, low melting solid (1.87 g, 72%); $[\alpha]_D^{20}$ −28.0 (*c* 2, MeOH, lit. −32.3,[29] *c* 1.84, MeOH); δ_H (400 MHz, $CDCl_3$): 1.14 (3H, s, CH_3), 1.18 (3H, s, CH_3), 1.60–1.82 (4H, m, 2 × CH_2), 2.84 (2H, br s, N*H* & O*H*), 2.90–3.05 (3H, m, CH_2 & C*H*); δ_C (100 MHz, $CDCl_3$): 25.2 (CH_3), 26.1 (CH_2), 26.3 (CH_2), 28.6 (CH_3), 47.0 (CH_2), 67.0 (*C*H), 70.3 (*C*); Data was in accordance with the literature.

(*S*)-[2-(2-Hydroxypropan-2-yl)pyrrolidin-1-yl](1-methyl-1*H*-imidazol-2-yl)methanone 21

(*S*)-α,α-Dimethyl-2-pyrrolinol **19** (1.29 g, 10 mmol) was dissolved in toluene (10 mL) and NaH (60% dispersion in mineral oil, 600 mg, 15 mmol) was added at rt. After stirring for 30 min, ethyl 1-methylimidazole-2-carboxylate **20** (1.69 g, 11 mmol) was added. The resulting reaction mixture was slowly warmed to 70 °C and stirred for 40 h. The reaction was cooled to rt, quenched by addition of water (20 mL) and extracted with ethyl acetate (3 × 30 mL). The combined organic phases were dried over $MgSO_4$. After filtration, the filtrate was evaporated and purified by chromatography on silica gel [50%–100% ethyl acetate in petroleum ether (40–60)] to yield the product **21** (0.896 g, 39%) as a white solid; m.p. 84–86 °C; $[\alpha]_D^{20}$ −124 (*c* 1.1, $CHCl_3$); (Found: C, 60.70; H, 7.98; N, 17.70. $C_{12}H_{19}N_3O_2$ requires C, 60.74; H, 8.07, N, 17.71%); ν_{max} (thin film) 3353 (br m), 2974 (m), 1607 (s), 1455 (s); δ_H (500 MHz, DMSO-d_6, 100 °C): 1.07 [6H, s, 2 × CH_3], 1.65–1.70 (1H, m, C*H*H), 1.89–1.95 (3H, m, CH_2 & C*H*H), 3.49–3.54 (1H, m, C*H*H), 3.79 (3H, s, CH_3), 3.97–4.03 (1H, m, C*H*H), 4.42–4.62 (1H, br m, O*H*), 4.71 (1H, br s, C*H*), 6.95 (1H, s, ArC*H*), 7.19 (1H, s,

ArC*H*); δ_C (126 MHz, DMSO-d_6, 100 °C): 23.4 (br, *C*H_2), 25.6 (*C*H2), 25.7 (*C*H_3), 26.9 (*C*H_3), 33.8 (*C*H_3), 48.7 (br *C*H_2), 65.2 (*C*H), 72.4 (*C*), 123.5 (Ar*C*H), 126.1 (Ar*C*H), 140.4 (Ar*C*), 160.4 (*C*O); HRMS (ES$^+$ TOF): found 238.1556 $[M + H]^+$; $C_{12}H_{20}N_3O_2$ requires 238.1550.

(*S*)-[2-(Hydroxydiphenylmethyl)pyrrolidin-1-yl](pyridin-2-yl) methanone 23

Oxalyl chloride (1.32 mL, 15 mmol) was added dropwise to a solution of picolinic acid (615 mg, 5 mmol) in DCM (15 mL). The resulting mixture was stirred at rt for 4 h, followed by evaporation to give a black solid. DCM (20 mL) was added and the suspension transferred into a solution of (*S*)-α,α-diphenylprolinol **13** (1.02 g, 4 mmol) in toluene (20 mL) and the resulting mixture stirred at rt overnight. The reaction was quenched by aqueous ammonium chloride (20 mL) and extracted with ethyl acetate (3 × 20 mL). The combined organic extracts were dried over Na_2SO_4, filtered, evaporated under reduced pressure, and the residue purified by chromatography on silica gel [20%–100% ethyl acetate in petroleum ether (40–60)] to yield the product **23** as white solid (950 mg, 66%); m.p. 129–131 °C (not reported in literature); $[\alpha]_D^{20}$ −118.7 (*c* 0.8, $CHCl_3$, not reported in literature); ν_{max} (thin film) 3058 (w), 2989 (w), 1608 (s), 1565 (s); δ_H (500 MHz, DMSO-d_6, 100 °C): 1.63–1.80 (2H, m, C*H*$_2$), 1.92–1.98 (1H, m, C*H*H), 2.05–2.12 (1H, m, C*H*H), 3.47–3.52 (1H, m, C*H*H), 3.65 (1H, br s, C*H*H), 5.72 (1H, br s, O*H*), 5.85 (1H, br s, C*H*), 7.06–7.26 (7H, m, ArC*H*), 7.32–7.35 (3H, m, ArC*H*), 7.48 (2H, d, *J* 7.6, ArC*H*), 7.69 (1H, br s, ArC*H*), 8.48 (1H, d, *J* 3.9, ArC*H*); δ_C (126 MHz, d_6-DMSO, 100 °C): 22.7 (br, *C*H_2), 27.4 (*C*H_2), 48.6 (br, *C*H_2), 63.9 (*C*H), 81.0 (*C*), 122.8 (Ar*C*H), 123.7 (Ar*C*H), 125.8 (2 × Ar*C*H), 126.1 (2 × Ar*C*H), 126.5 (2 × Ar*C*H), 126.7 (2 × Ar*C*H), 127.0 (2 × Ar*C*H), 136.1 (Ar*C*H), 145.0 (Ar*C*), 145.4 (Ar*C*), 146.9 (br, Ar*C*), 154.0 (Ar*C*H), 166.9 (br, *C*O); HRMS (ES$^+$ TOF): found 359.1769 $[M + H]^+$; $C_{23}H_{23}N_2O_2$ requires 359.1760.

(*S*)-[2-(Methoxydiphenylmethyl)pyrrolidin-1-yl](1-methyl-1*H*-imidazol-2-yl)methanone 26

NaH (60% dispersion in mineral oil, 44 mg, 1.1 mmol) was added to a solution of hydroxy catalyst **17** (361 mg, 1 mmol) in THF (10 mL). After stirring for 20 min at rt, MeI (156 mg, 1.1 mmol) was added dropwise at the same temperature and then stirred overnight. The resulting mixture was quenched with saturated aqueous ammonium chloride (10 mL). The organic phase was separated and the aqueous phase was extracted with DCM (3 × 10 mL). The combined organic extracts were dried over $MgSO_4$. After filtration and evaporation, the residue was purified by chromatography on silica gel [20%–50% ethyl acetate in petroleum ether (40–60)] to yield the product **26** as a white foam as a 4.6 : 1 mixture of two rotamers A and B (0.21 g, 56%); m.p. 93–95 °C; $[\alpha]_D^{20}$ −68 (*c* 0.5, $CHCl_3$); ν_{max} (thin film) 2927 (w), 1624 (s), 1524 (m), 1463 (s); δ_H (400 MHz, $CDCl_3$, rotamer A): 1.03–1.16 (1H, m, C*H*H), 1.57–1.68 (1H, m, C*H*H), 1.98–2.05 (1H, m, C*H*H), 2.25–2.48 (2H, m, C*H*$_2$), 2.38 (3H, s, C*H*$_3$), 3.54–3.61 (1H, m, C*H*), 3.79 (3H, s, C*H*$_3$), 6.31 (1H, d, *J* 8.9, C*H*), 6.79 (1H, d, *J* 0.9, ArC*H*), 6.95 (1H, d, *J* 0.9, ArC*H*), 7.26–7.36 (7H, m, ArC*H*), 7.46–7.52 (1H, m, ArC*H*); δ_H (400 MHz, $CDCl_3$, rotamer B): 1.03–1.16 (1H, m, C*H*H), 1.45–1.53 (1H, m, C*H*H), 1.98–2.05 (1H, m, C*H*H), 2.95–3.02 (1H, m, C*H*H), 3.00 (3H, s, C*H*$_3$), 3.70–3.76 (1H, m, C*H*H), 3.86 (3H, s, C*H*$_3$), 5.72 (1H, dd, *J* 8.7, 3.1, C*H*), 6.89 (1H, s, ArC*H*), 7.07 (1H, s, ArC*H*), 7.26–7.36 (8H, m, ArC*H*); δ_C (100 MHz, $CDCl_3$, rotamer A): 21.8 (*C*H_2), 27.6 (*C*H_2), 34.2 (*C*H_3), 47.4 (*C*H_2), 51.8 (*C*H_3), 63.5 (*C*H), 86.8 (*C*), 122.4 (Ar*C*H), 126.6 (Ar*C*H), 127.6 (3 × Ar*C*H), 127.7 (3 × Ar*C*H), 129.4 (2 × Ar*C*H), 130.0 (2 × Ar*C*H), 138.8 (ArC), 139.7 (ArC), 142.6 (ArC), 161.2 (*C*O); δ_C (100 MHz, $CDCl_3$, rotamer B): 23.9 (*C*H_2), 26.6 (*C*H_2), 29.7 (*C*H_2), 35.4 (*C*H_3), 50.7 (*C*H_2), 52.5 (*C*H_3), 60.4 (*C*H), 86.7 (*C*), 123.9 (Ar*C*H), 127.4 (2 × Ar*C*H), 127.5 (2 × Ar*C*H), 127.8 (3 × Ar*C*H), 129.6 (3 × Ar*C*H), 129.9 (ArCH), 140.1 (Ar*C*), 140.9 (Ar*C*), 141.2 (Ar*C*), 161.2 (*C*O); HRMS (ES$^+$ TOF): found 376.2023 $[M + H]^+$; $C_{23}H_{26}N_3O_2$ requires 376.2025.

(*S*)-[2-(Methoxydiphenylmethyl)pyrrolidin-1-yl](pyridin-2-yl) methanone 27

NaH (60% dispersion in mineral oil, 80 mg, 2 mmol) was added to a solution of alcohol **23** (358 mg, 1 mmol) in THF (8 mL). After stirring for 15 min at rt, MeI (284 mg, 2 mmol) was added dropwise at rt and left to stir overnight. The resulting mixture was quenched with saturated aqueous ammonium chloride (20 mL). The organic phase was separated and the aqueous phase was extracted with ethyl acetate (3 × 15 mL). The combined organic extracts were dried over Na_2SO_4, filtered, evaporated, and the resulting residue purified by chromatography on silica gel [10%–100% ethyl acetate in petroleum ether (40–60)] to yield the product **27** as a yellow solid as a 2 : 1 mixture of rotamers A and B (308 mg, 83%); m.p. 104–106 °C; $[\alpha]_D^{20}$ −154 (*c* 1.0, $CHCl_3$); ν_{max} (thin film) 3056 (m), 2961 (m), 1626 (s), 1587 (s), 1556 (s); δ_H (400 MHz, $CDCl_3$, rotamer A): 1.04–1.16 (1H, m, C*H*H), 1.59–1.70 (1H, m, C*H*H), 1.94–2.01 (1H, m, C*H*H), 2.31 (3H, s, C*H*$_3$), 2.37–2.45 (2H, m, C*H*$_2$), 3.65–3.72 (1H, m, C*H*), 6.20 (1H, dd, *J* 9.2, 1.6, C*H*), 7.25–7.39 (9H, m, ArC*H*), 7.52 (1H, d, *J* 9.1, *ArCH*), 7.60 (1H, d, *J* 6.7, *ArCH*), 7.59–7.78 (2H, m, ArC*H*), 8.54 (1H, d, *J* 4.8, *ArCH*); δ_H (400 MHz, $CDCl_3$, rotamer B): 1.04–1.16 (1H, m, C*H*), 1.44–1.55 (1H, m, C*H*), 2.02–2.11 (1H, m, C*H*), 2.13–2.23 (1H, m, C*H*), 2.71–2.78 (1H, m, C*H*), 3.07 (3H, s, C*H*$_3$), 3.15–3.21 (1H, m, C*H*), 5.80 (1H, dd, *J* 9.1, 3.2, C*H*), 7.25–7.39 (11H, m, ArC*H*), 7.59–7.78 (2H, m, ArC*H*), 8.65 (1H, d, *J* 4.6, *ArCH*); δ_C (100 MHz, $CDCl_3$, rotamer A): 21.6 (*C*H_2), 27.8 (*C*H_2), 47.7 (*C*H_2), 50.7 (*C*H), 64.0 (*C*H_3), 87.0 (*C*), 123.7 (Ar*C*H), 124.3 (Ar*C*H), 127.3 (2 × Ar*C*H), 127.6 (Ar*C*H), 127.7 (2 × Ar*C*H), 127.8 (Ar*C*H), 127.9 (Ar*C*H), 129.6 (Ar*C*H), 129.8 (Ar*C*H), 129.9 (Ar*C*H), 130.0 (Ar*C*H), 138.4 (Ar*C*), 138.6 (Ar*C*), 146.9 (Ar*C*H), 156.6 (Ar*C*), 168.5 (*C*O); δ_C (100 MHz, $CDCl_3$, rotamer B): 24.0 (*C*H_2), 26.9 (*C*H_2), 50.6 (*C*H_2), 52.3 (*C*H), 59.8 (*C*H_3), 86.6 (*C*), 124.5 (Ar*C*H), 127.3 (Ar*C*H), 127.6 (Ar*C*H), 127.7 (2 × Ar*C*H), 127.8 (Ar*C*H), 127.9 (Ar*C*H), 129.6 (Ar*C*H), 129.8 (Ar*C*H), 129.9 (Ar*C*H), 130.0 (Ar*C*H), 136.4 (2 × Ar*C*H), 140.5 (Ar*C*), 141.9 (Ar*C*), 148.7 (Ar*C*H), 155.0 (Ar*C*), 169.1 (*C*O); HRMS (ES$^+$ TOF): found 373.1917 $[M + H]^+$; $C_{24}H_{25}N_2O_2$ requires 373.1916.

(*S*)-*N*-[1-Phenylethyl]-4-fluoroaniline 34[26]

Obtained using general procedure A with ketimine **29**, employing catalyst **17** (1 mol%, 96% conversion, 87% ee) or catalyst **26** (0.1 mol%, 95% conversion, 86% ee) as a light yellow oil; $[\alpha]_D^{20}$ +23.8 (*c* 1.05, $CHCl_3$, 87% ee, lit.[26] −16.8, *c* 1.0, $CHCl_3$, 84% ee for *R*-enantiomer); δ_H (400 MHz, $CDCl_3$): 1.52 (3H, d, *J* 6.6, C*H*$_3$), 4.03 (1H, br s, N*H*), 4.45 (1H, q, *J* 6.6, C*H*), 6.43–6.47 (2H, m, ArC*H*), 6.79–6.84 (2H, m, ArC*H*), 7.23–7.28 (1H, m, ArC*H*), 7.32–7.38 (4H, m, ArC*H*); δ_C (101 MHz, $CDCl_3$): 25.1 (*C*H$_3$), 54.1 (*C*H), 114.1 (d, J_{C-F} 6.9, Ar*C*H), 115.5 (d, J_{C-F} 22.2, Ar*C*H), 125.9 (Ar*C*H), 127.0 (Ar*C*H), 128.8 (Ar*C*H), 143.7 (Ar*C*), 145.1 (Ar*C*), 155.5 (d, J_{C-F} 234.6, Ar*C*); HPLC (Kromasil 3-Cellucoat OD, hexane/i-PrOH = 99/1, flow rate = 1.0 mL min^{-1}, 254 nm): (*R*) enantiomer t_R = 6.9 min, (*S*) enantiomer t_R = 7.8 min.

(*S*)-*N*-[1-(4′-Methoxyphenyl)ethyl]-4-methoxyaniline 35[16]

Obtained using general procedure A with ketimine **30**, employing catalyst **26** (0.1 mol%, 97% conversion, 84% ee) as a white solid; m.p. 93–95 °C (not reported in literature); $[\alpha]_D^{20}$ −14.5 (*c* 0.96, $CHCl_3$, 81% ee, lit. −15.5,[16] *c* 1.1, $CHCl_3$, 85% ee); δ_H (250 MHz, $CDCl_3$): 1.49 (3H, d, *J* 6.6, C*H*$_3$), 3.72 (3H, s, C*H*$_3$), 3.76 (1H, br s, N*H*), 3.80 (3H, s, C*H*$_3$), 4.39 (1H, q, *J* 6.6, C*H*), 6.49 [2H, $(AX)_2$, ArC*H*], 6.71 [2H, $(AX)_2$, ArC*H*], 6.87 [2H, $(AX)_2$, ArC*H*], 7.29 [2H, $(AX)_2$, ArC*H*]; δ_C (63 MHz, $CDCl_3$): 25.1 (*C*H$_3$), 53.7 (*C*H$_3$), 55.3, (*C*H$_3$), 55.8 (*C*H$_3$), 114.0 (2 × Ar*C*H), 114.6 (2 × Ar*C*H), 114.8 (2 × Ar*C*H), 127.0 (2 × Ar*C*H), 137.6 (Ar*C*), 141.7 (Ar*C*), 151.9 (Ar*C*), 158.5 (Ar*C*); HPLC (Phenomenex Lux 3 μm Cellulose-1, hexane/i-PrOH = 90/10, flow rate = 1.0 mL min^{-1}, 254 nm): (*R*) enantiomer t_R = 9.1 min, (*S*) enantiomer t_R = 10.0 min.

(*S*)-*N*-[1-(4′-Nitrophenyl)ethyl]-4-methoxyaniline 36[16]

Obtained using general procedure A with ketimine 31, employing catalyst **26** (0.1 mol%, 98% conversion, 84% ee) as a brown oil; $[\alpha]_D^{20}$ −30.8 (*c* 1.0, $CHCl_3$, 84% ee, lit. −25.9,[16] *c* 0.54, $CHCl_3$, 86% ee); δ_H (400 MHz, $CDCl_3$): 1.55 (3H, d, *J* 6.8, C*H*$_3$), 3.72 (3H, s, C*H*$_3$), 3.93 (1H, br s, N*H*), 4.53 (1H, q, *J* 6.8, C*H*), 6.43 (2H, d, *J* 8.2, ArC*H*), 6.72 (2H, d, *J* 8.2, ArC*H*), 7.57 (2H, d, *J* 8.8, ArC*H*), 8.20 (2H, d, *J* 8.8, ArC*H*); δ_C (101 MHz, $CDCl_3$): 25.0 (*C*H$_3$), 54.0 (*C*H$_3$), 55.7 (*C*H), 114.5 (2 × Ar*C*H), 114.8 (2 × Ar*C*H), 124.1 (2 × Ar*C*H), 126.8 (2 × Ar*C*H), 140.8 (Ar*C*), 147.0 (Ar*C*), 152.3 (Ar*C*), 153.6 (Ar*C*); HPLC (Phenomenex Lux 3 μm Cellulose-1, hexane/i-PrOH = 90/10, flow rate = 1.0 mL min^{-1}, 254 nm): (*R*) enantiomer t_R = 28.3 min, (*S*) enantiomer t_R = 31.8 min.

(*S*)-*N*-[1-(Thiophen-2-yl)ethyl]-4-methoxyaniline 37[17]

Obtained using general procedure A with ketimine **32**, employing catalyst **26** (0.1 mol%, 77% conversion, 80% ee) as a yellow oil; $[\alpha]_D^{20}$ −8.0 (*c* 1.0, $CHCl_3$, 79% ee, lit.[17] −8.0, *c* 1.0, $CHCl_3$, 79% ee); δ_H (250 MHz, $CDCl_3$): 1.63 (3H, d, *J* 6.6, C*H*$_3$), 3.75 (3H, s, C*H*$_3$), 4.76 (1H, q, *J* 6.6, C*H*), 6.62 [2H, $(AX)_2$, ArC*H*], 6.75 [2H, $(AX)_2$, ArC*H*], 6.94–6.98 (2H, m, ArC*H*), 7.18 (1H, dd, *J* 4.7, 1.6, ArC*H*); δ_C (63 MHz, $CDCl_3$): 24.8 (*C*H$_3$), 50.6 (*C*H$_3$), 55.8 (*C*H), 114.9 (2 × Ar*C*H), 115.2 (2 × Ar*C*H), 123.0 (Ar*C*H), 123.6 (Ar*C*H), 126.7 (Ar*C*H), 141.2 (Ar*C*), 150.6 (Ar*C*), 152.5 (Ar*C*); HPLC (Phenomenex Lux 3 μm Cellulose-1, hexane/i-PrOH = 98/2, flow rate = 1.0 mL min^{-1}, 254 nm): (*R*) enantiomer t_R = 15.1 min, (*S*) enantiomer t_R = 17.3 min.

(*S*)-*N*-[1-(Naphthalen-2-yl)ethyl]-4-methoxyaniline 38[16]

Obtained using general procedure A with ketimine **33**, employing catalyst **26** (0.1 mol%, 99% conversion, 92% ee) as a light yellow solid; m.p. 96–98 °C (lit.[16] 95–96 °C); $[\alpha]_D^{20}$ −24.0 (*c* 1.0, $CHCl_3$, 85% ee, lit.[16] −26.0, *c* 1.0, $CHCl_3$, 86% ee); δ_H (250 MHz, $CDCl_3$): 1.59 (3H, d, *J* 6.9, C*H*$_3$), 3.70 (3H, s, C*H*$_3$), 3.90 (1H, br s, N*H*), 4.59 (1H, q, *J* 6.9, C*H*), 6.53 [2H, $(AX)_2$, ArC*H*], 6.71 [2H, $(AX)_2$, ArC*H*], 7.42–7.55 (3H, m, ArC*H*), 7.80–7.86 (4H, m, ArC*H*); δ_C (63 MHz, $CDCl_3$): 25.2 (*C*H$_3$), 54.6 (*C*H$_3$), 55.8 (*C*H), 114.7 (Ar*C*H), 114.8 (Ar*C*H), 124.4 (Ar*C*H), 124.5 (Ar*C*H), 125.5 (Ar*C*H), 126.0 (Ar*C*H), 127.7 (Ar*C*H), 127.9 (Ar*C*H), 128.5 (Ar*C*H), 132.8 (Ar*C*), 133.7 (Ar*C*), 141.7 (Ar*C*), 143.1 (Ar*C*), 152.0 (Ar*C*); HPLC (Phenomenex Lux 3 μm Cellulose-1, hexane/i-PrOH = 90/10, flow rate = 1.0 mL min^{-1}, 254 nm): (*R*) enantiomer t_R = 10.1 min, (*S*) enantiomer t_R = 12.0 min.

Acknowledgements

We thank The University of Sheffield (XL and FT) and EPSRC (EP/K007955/1 – ATR) for funding.

Notes and references

1 F. Iwasaki, O. Onomura, K. Mishima, T. Kanematsu, T. Maki and Y. Matsumura, *Tetrahedron Lett.*, 2001, **42**, 2525–2527.
2 S. Guizzetti and M. Benaglia, *Eur. J. Org. Chem.*, 2010, 5529–5541.
3 S. Jones and C. J. A. Warner, *Org. Biomol. Chem.*, 2012, **10**, 2189–2200.
4 A. V. Malkov, A. Mariani, K. N. MacDougall and P. Kočovský, Pavel, *Org. Lett.*, 2004, **6**, 2253–2256.
5 Z. Wang, X. Ye, S. Wei, P. Wu, A. Zhang and J. Sun, *Org. Lett.*, 2006, **8**, 999–1001.
6 C. Baudequin, D. Chaturvedi and S. B. Tsogoeva, *Eur. J. Org. Chem.*, 2007, 2623–2629.
7 Y.-C. Xiao, C. Wang, Y. Yao, J. Sun and Y.-C. Chen, *Angew. Chem., Int. Ed.*, 2011, **50**, 10661–10664.
8 D. Pei, Z. Wang, S. Wei, Y. Zhang and J. Sun, *Org. Lett.*, 2006, **8**, 5913–5915.
9 D. Pei, Y. Zhang, S. Wei, M. Wang and J. Sun, *Adv. Synth. Catal.*, 2008, **350**, 619–623.
10 S. Guizzetti, M. Benaglia, F. Cozzi and R. Annunziata, *Tetrahedron*, 2009, **65**, 6354–6363.
11 H. Zheng, J. Deng, W. Lin and X. Zhang, *Tetrahedron Lett.*, 2007, **48**, 7934–7937.

12 O. Onomura, Y. Kouchi, F. Iwasaki and Y. Matsumura, *Tetrahedron Lett.*, 2006, **47**, 3751–3754.
13 C. J. A. Warner, A. T. Reeder and S. Jones, *Tetrahedron: Asymmetry*, 2016, **27**, 136–141.
14 M. Bonsignore, M. Benaglia, R. Annunziata and G. Celentano, *Synlett*, 2011, 1085–1088.
15 M. Sugiura, M. Kumahara and M. Nakajima, *Chem. Commun.*, 2009, 3585–3587.
16 F.-M. Gautier, S. Jones and S. J. Martin, *Org. Biomol. Chem.*, 2009, **7**, 229–231.
17 F.-M. Gautier, S. Jones, X. Li and S. J. Martin, *Org. Biomol. Chem.*, 2011, **9**, 7860–7868.
18 Z. Zhang, P. Rooshenas, H. Hausmann and P. Schreiner, *Synthesis*, 2009, 1531–1544.
19 A. V. Malkov, K. Vranková, S. Stončius and P. Kočovský, *J. Org. Chem.*, 2009, **74**, 5839–5849.
20 R. E. Cowley, R. P. Bontchev, E. N. Duesler and J. M. Smith, *Inorg. Chem.*, 2006, **45**, 9771–9779.
21 M. Braun, *Angew. Chem., Int. Ed.*, 2012, **51**, 2550–2562.
22 S. El-Fayyoumy, M. H. Todd and C. J. Richards, *Beilstein J. Org. Chem.*, 2009, **5**, 67.
23 M. Hagemann, A. Mix, R. J. F. Berger, T. Pape and N. W. Mitzel, *Inorg. Chem.*, 2008, **47**, 10554–10564.
24 A. V. Malkov, S. Stončius, K. Vrankova, M. Arndt and P. Kočovský, *Chem. – Eur. J.*, 2008, **14**, 8082–8085.
25 S. Jones and X. Li, *Tetrahedron*, 2012, **68**, 5522–5532.
26 T. Imamoto, N. Iwadate and K. Yoshida, *Org. Lett.*, 2006, **8**, 2289–2292.
27 R. I. Ngochindo, *J. Chem. Soc., Perkin Trans. 1*, 1990, 1645–1648.
28 P. A. Shirley, D. A. Gross and B. H. Roussel, *J. Org. Chem.*, 1955, **20**, 225–231.
29 K. Nakayama and W. J. Thompson, *J. Am. Chem. Soc.*, 1990, **112**, 6936–6942.